The effect of the Leeuwin Current on phytoplankton biomass and production off Southwestern Australia

J. Anthony Koslow, Stephane Pesant, Ming Feng, Alan Pearce, Peter Fearns, Thomas Moore, Richard Matear, Anya Waite

▶ **To cite this version:**

J. Anthony Koslow, Stephane Pesant, Ming Feng, Alan Pearce, Peter Fearns, et al.. The effect of the Leeuwin Current on phytoplankton biomass and production off Southwestern Australia. Journal of Geophysical Research. Oceans, 2008, 113, 10.1029/2007JC004102 . hal-04110509

HAL Id: hal-04110509
https://hal.science/hal-04110509v1

Submitted on 31 May 2023

HAL is a multi-disciplinary open access archive for the deposit and dissemination of scientific research documents, whether they are published or not. The documents may come from teaching and research institutions in France or abroad, or from public or private research centers.

L'archive ouverte pluridisciplinaire **HAL**, est destinée au dépôt et à la diffusion de documents scientifiques de niveau recherche, publiés ou non, émanant des établissements d'enseignement et de recherche français ou étrangers, des laboratoires publics ou privés.

Copyright

The effect of the Leeuwin Current on phytoplankton biomass and production off Southwestern Australia

J. Anthony Koslow,[1,2] Stephane Pesant,[3,4] Ming Feng,[1] Alan Pearce,[1] Peter Fearns,[1] Thomas Moore,[5] Richard Matear,[5] and Anya Waite[3]

Received 13 January 2007; revised 6 January 2008; accepted 27 February 2008; published 30 July 2008.

[1] Unlike most eastern boundary currents, the Leeuwin Current off the west coast of Australia flows poleward and is therefore warm, nutrient-poor and suppresses upwelling. As a result, the waters off Western Australia are relatively oligotrophic. Primary productivity and concentrations of chlorophyll are particularly low in summer, when the water column is stratified and most chlorophyll is concentrated in a layer above the nutricline at approximately 100 m depth. The phytoplankton blooms in late autumn and winter, coinciding with the period of strongest Leeuwin flow. The bloom in winter is maintained by cooling and storms, which promote convective mixing of the upper water column and a shoaling of the nutricline and chlorophyll maximum layer. However, the late autumn bloom coincides with the initial intensification of the Leeuwin Current. Eddies and meanders spin up just beyond the shelf break, and Leeuwin Current water was observed at this time to destratify the water column and flood the shelf with relatively nutrient-rich water. Several potential sources for the nutrients are proposed: upwelling by the eddies and meanders as they induce cross-shelf motions; advection from the north, where the nutricline is shallower; and seasonal cooling.

Citation: Koslow, J. A., S. Pesant, M. Feng, A. Pearce, P. Fearns, T. Moore, R. Matear, and A. Waite (2008), The effect of the Leeuwin Current on phytoplankton biomass and production off Southwestern Australia, *J. Geophys. Res.*, *113*, C07050, doi:10.1029/2007JC004102.

1. Introduction

[2] The oceanography off the west coast of Australia is dominated by the Leeuwin Current, an anomalous poleward-flowing eastern boundary current that extends between Northwest Cape (22°S) and Cape Leeuwin (35°S), and in winter can be traced along the south coast to Tasmania [*Ridgway and Condie*, 2004]. First described in 1980 [*Cresswell and Golding*, 1980], the Leeuwin Current is driven by an alongshore pressure gradient set up by the Indonesian Throughflow between the Pacific and Indian Oceans and surface heat loss at higher latitudes [*Godfrey and Ridgway*, 1985; *Cresswell*, 1991]. A relatively narrow, shallow but intense current, the Leeuwin is limited to the upper 250–300 m, with its core over the upper continental slope, between the shelf break and about 100 km offshore. Seasonally, flow of the Leeuwin Current is weakest in the austral summer, when it opposes strong southerly monsoonal winds (December–February). Flow increases in late autumn (April–May), when the southerlies decline, and continues to flow strongly through the austral winter (June–August) [*Godfrey and Ridgway*, 1985; *Feng et al.*, 2003]. Annual mean flow is on the order of 20 cm s^{-1}, but flow during late autumn and early winter often exceeds 50 cm s^{-1}, with transport on the order of 2 Sv in summer and 5 Sv in autumn and winter [*Smith et al.*, 1991; *Feng et al.*, 2003].

[3] The Leeuwin Current, whose poleward flow promotes downwelling, shares several characteristics with western boundary currents. Leeuwin waters, like those of western boundary currents such as the Gulf Stream, are relatively warm and low in nutrient, and pelagic productivity is dramatically lower than in the major eastern boundary currents. The commercial catch of pilchard (*Sardinops sagax*), the dominant pelagic plankton-feeder off Western Australia, has been less than 4000 tons off the west coast, 2–3 orders of magnitude lower than in productive eastern boundary current systems [*Pearce*, 1991; *Lenanton et al.*, 1991; *Gaughan and Leary*, 2003].

[4] Another distinct feature of the Leeuwin Current is its eddy kinetic energy, which is substantially higher than that of other eastern boundary currents [*Feng et al.*, 2005], though less than that of the major western boundary currents. Meanders and eddies spin up during the autumn-winter period and often continue to evolve through winter, to be either reabsorbed or shed into the interior of the eastern Indian Ocean and drift westward [*Morrow et al.*, 2003; *Fang and Morrow*, 2003]. Western boundary current

[1]CSIRO Marine and Atmospheric Research, Wembley, WA, Australia.
[2]Now at Integrative Oceanography Division, Scripps Institution of Oceanography, University of California, San Diego, La Jolla, California, USA.
[3]School of Environmental Systems Engineering, University of Western Australia, Crawley, WA, Australia.
[4]Now at Observatoire Océanologique, Laboratoire d'Océanographie de Villefranche (LOV)-UMR 7093, Villefranche-sur-Mer, France.
[5]CSIRO Marine and Atmospheric Research, Hobart, Tas, Australia.

Copyright 2008 by the American Geophysical Union.
0148-0227/08/2007JC004102

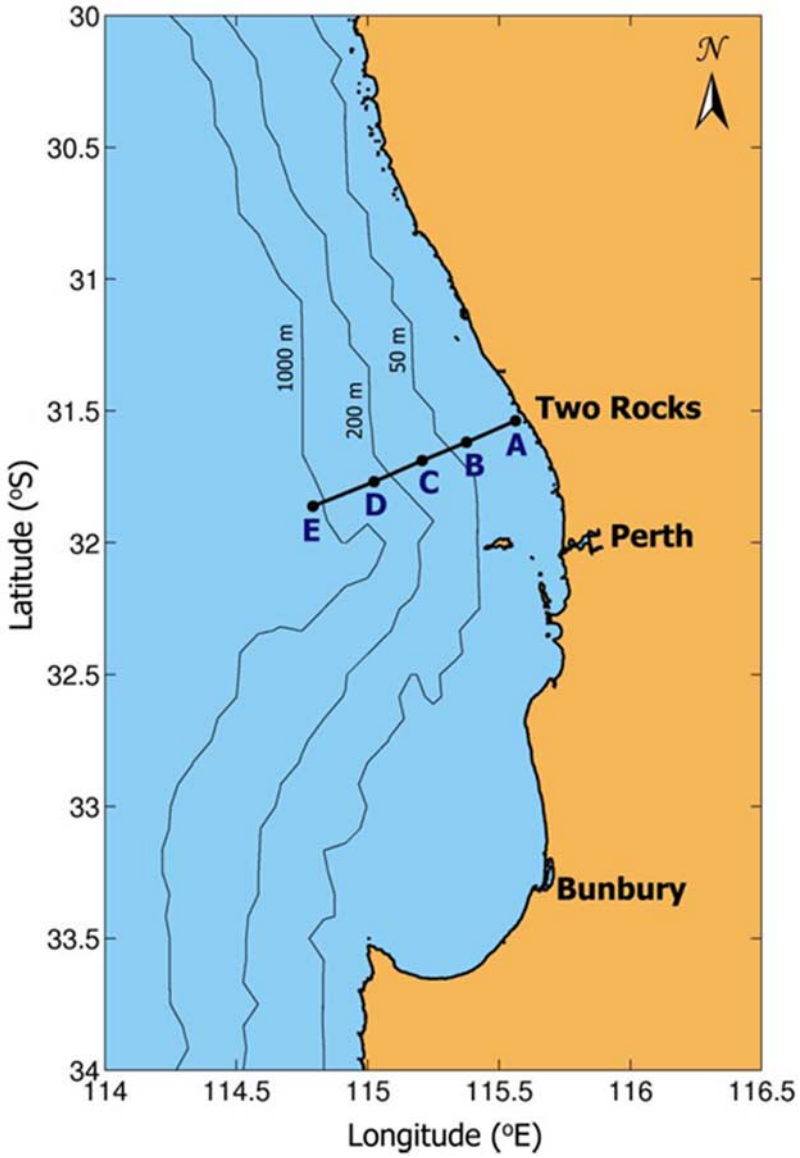

Figure 1a. Location of the Two Rocks transect north of Perth.

eddies and meanders have been shown to contribute significantly to the productivity of the continental shelves off the southeastern USA [*Yoder et al.*, 1981; *Lee and Atkinson*, 1983; *Lee et al.*, 1989, 1991], Brazil [*Campos et al.*, 2000], Japan [*Kimura et al.*, 1997], and eastern Australia [*Tranter et al.*, 1986; *Harris et al.*, 1987], but the impact of eddies off the coast of Western Australia on shelf productivity has not been previously examined.

[5] On the other hand, the Leeuwin Current, like the Peru and California Currents, responds to the ENSO cycle, because of the existence of the equatorial and coastal wave guidance off northwest and west Australian coast, and hence to the trans-Pacific wind field [*Birol and Morrow*, 2001; *Potemra*, 2001]. Sea level along the coast provides a good index of Leeuwin Current transport [*Feng et al.*, 2003].

[6] Recruitment to several fisheries in Western Australia, including the Australian salmon (*Arripis truttaceus*), Australian herring (*A. georgianus*), and pilchard, appears linked to the strength of the Leeuwin Current [*Lenanton et al.*, 1991]. The most notable correlation, however, is with recruitment to the western rock lobster fishery, Australia's most valuable single-species fishery. Recruitment to the population is determined during the lobster's pelagic phyllosoma period. Interestingly, although the Leeuwin is generally believed responsible for the low pelagic productivity off the west coast of Australia, rock lobster recruitment is positively correlated with the strength of the Leeuwin Current, with poor recruitment during El Nino years characterized by a weak Leeuwin Current [*Caputi et al.*, 2001]. An advection-based model of the larval dynamics of the western rock lobster indicated no relationship between the ENSO cycle and larval drift to their inshore nursery area, with the suggestion that the flow of the Leeuwin Current may in some way be positively linked to regional productivity [*Griffin et al.*, 2001].

[7] The continental shelf off southwestern Western Australia is characterized by a coastal "lagoon" created by ancient reefs several kilometers off the coast; a shallow-

21562202c, 2008, C7, Downloaded from https://agupubs.onlinelibrary.wiley.com/doi/10.1029/2007JC004102 by Cochrane France, Wiley Online Library on [31/05/2023]. See the Terms and Conditions (https://onlinelibrary.wiley.com/terms-and-conditions) on Wiley Online Library for rules of use; OA articles are governed by the applicable Creative Commons License

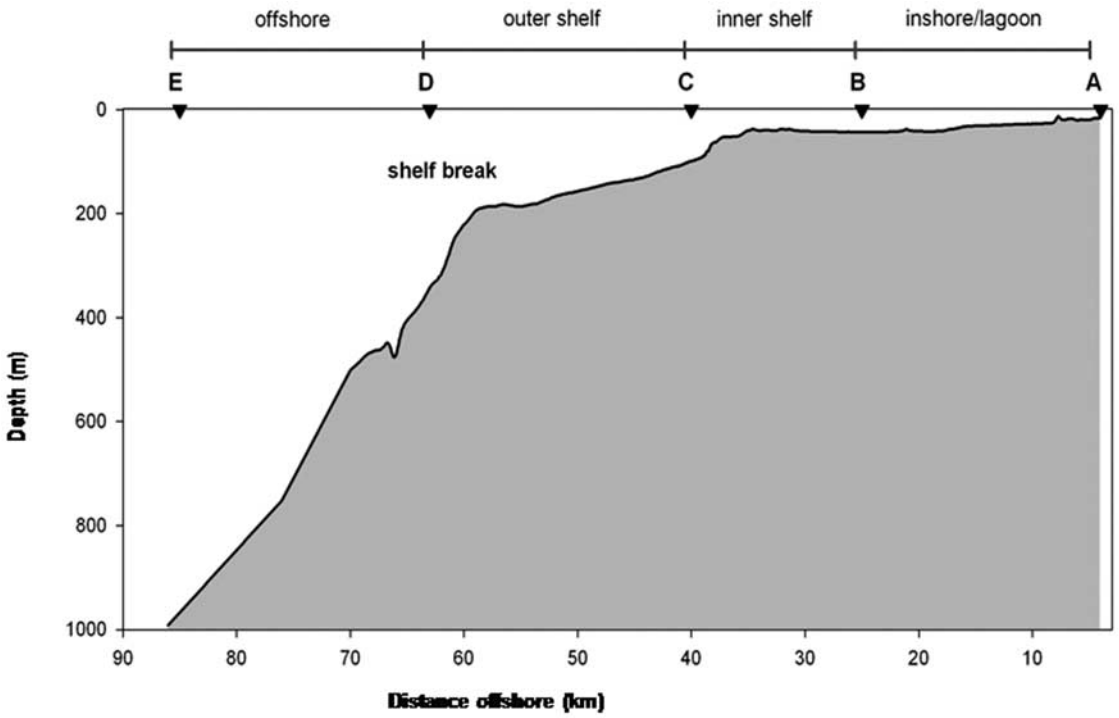

Figure 1b. Cross-shelf profile of the Two Rocks transect stations, A to E.

sloping inner shelf that extends to about 40 m depth, and a shelf break at 200–300 m depth. The continental shelf off Perth (32°S) is about 60 km wide. During summer, when the southerly winds are strongest and the Leeuwin Current is weakest, a counter-current known as the Capes Current flows northward over the continental shelf [*Pearce and Pattiaratchi*, 1999].

[8] The annual cycle of the plankton was described along an offshore meridional section along 110°E during the International Indian Ocean Expedition of 1962–1963 [*Tranter*, 1977] but is less well studied over the continental shelf and slope. *Longhurst* [1998] predicted that the seasonal cycle in the coastal zone off Western Australia would follow the canonical spring-bloom cycle observed in temperate shelf systems, as described by *Sverdrup* [1953], in which the bloom is a consequence of winter mixing of nutrients into the euphotic zone, followed by shoaling of the mixed layer and increased light in spring. More recent satellite observations across the shelf and Leeuwin Current indicate that chlorophyll levels are highest in winter [*Moore*, 2005; *Lourey et al.*, 2006], suggesting a subtropical plankton cycle, similar to that observed over the open ocean waters of the sub-tropical South Indian Ocean and most other sub-tropical ocean basins [*Yoder et al.*, 1993], although nearshore field observations have proved equivocal [*Pearce et al.*, 2000, 2006; *Thompson and Waite*, 2003]. The sub-tropical winter bloom is generally believed to be caused by breakdown of the seasonal thermocline, which injects nutrients into the upper mixed layer, combined with the relatively high solar irradiance at these latitudes in winter [*Longhurst*, 1998]. However, plankton production processes often differ markedly in coastal and shelf regions compared with those found over the open ocean.

[9] The aim of the present study is to characterize the seasonal cycle of plankton production across the continental shelf and within the Leeuwin Current off southwest Western Australia, and to assess its onshore-offshore variability and physical drivers. We carried this out through analysis of remotely sensed sea-surface temperature, ocean color, and sea-surface height data, combined with field measurements over a 3-year period along an onshore-offshore transect of the temperature and salinity characteristics of the water

Table 1. Location, Nominal Water Depth and Distance Offshore of the Two Rocks Transect Stations

Station	Environment	Latitude, °S	Longitude, °E	Depth, m	Distance Offshore, km
A	lagoon	31.5195	115.5980	15	4
AB		31.5363	115.5594	36	14
B	inner shelf	31.5772	115.4632	40	27
BC		31.6183	115.3652	50	32
C	outer shelf	31.6484	115.2956	100	40
CD		31.6799	115.2210	150	50
D	shelf break	31.7215	115.1230	300	61
DE		31.7650	115.0198	700	73
E	slope	31.8118	114.9092	1000	85

21562202c, 2008, C7, Downloaded from https://agupubs.onlinelibrary.wiley.com/doi/10.1029/2007JC004102 by Cochrane France, Wiley Online Library on [31/05/2023]. See the Terms and Conditions (https://onlinelibrary.wiley.com/terms-and-conditions) on Wiley Online Library for rules of use; OA articles are governed by the applicable Creative Commons License

Table 2. Summary of the Cruises Undertaken During the 3-Year Field Program Off Two Rocks, Western Australia

Voyage	Month	Year	Season	Vessel	Stations
MI200201	Feb	2002	summer	*Maritime Image*	A, B, C, E
MC200202	Mar	2002	fall	shark cat	A, B
MC200203	May	2002	fall	shark cat	A, B, C
NA200204	Aug	2002	winter	*Naturaliste*	A, B, C, D, E
MC200205	Nov	2002	spring	shark cat	A, B, C
MI200206	Dec	2002	summer	*Maritime Image*	A, B, C, D, E
MC200301	Jan	2003	summer	shark cat	A
NA200302	Feb	2003	summer	*Naturaliste*	A, B, C, D, E
MC200303a	Mar	2003	fall	shark cat	C
MC200303	Apr	2003	fall	shark cat	A, B, C
NA200304	Apr	2003	fall	*Naturaliste*	A, B, C, D, E
MC200305	Jun	2003	winter	shark cat	A, B, C
MC200306	Aug	2003	winter	shark cat	A
SS200307	Aug	2003	winter	*Southern Surveyor*	A, B, C, D, E
MC200308	Sep	2003	winter	shark cat	A, B, C
SS200309	Oct	2003	spring	*Southern Surveyor*	A, B, C, D, E
NA200311	Dec	2003	summer	*Naturaliste*	A, B, C, D, E
SS200401	Jan	2004	summer	*Southern Surveyor*	A, B, C, D, E
MC200402	Apr	2004	fall	shark cat	A, B, C
MI200403	Apr	2004	fall	*Maritime Image*	A, E
MC200404	Jun	2004	winter	shark cat	A, B, C
MI200405	Jul	2004	winter	*Maritime Image*	A, B, C, D, E
MC200406	Aug	2004	winter	shark cat	A, B, C
NA200407	Sep	2004	spring	*Naturaliste*	A, B, C, D, E
MC200408	Oct	2004	spring	shark cat	A, B, C
MC200409	Nov	2004	spring	shark cat	A, B, C
NA200410	Dec	2004	summer	*Naturaliste*	A, B, C, D, E

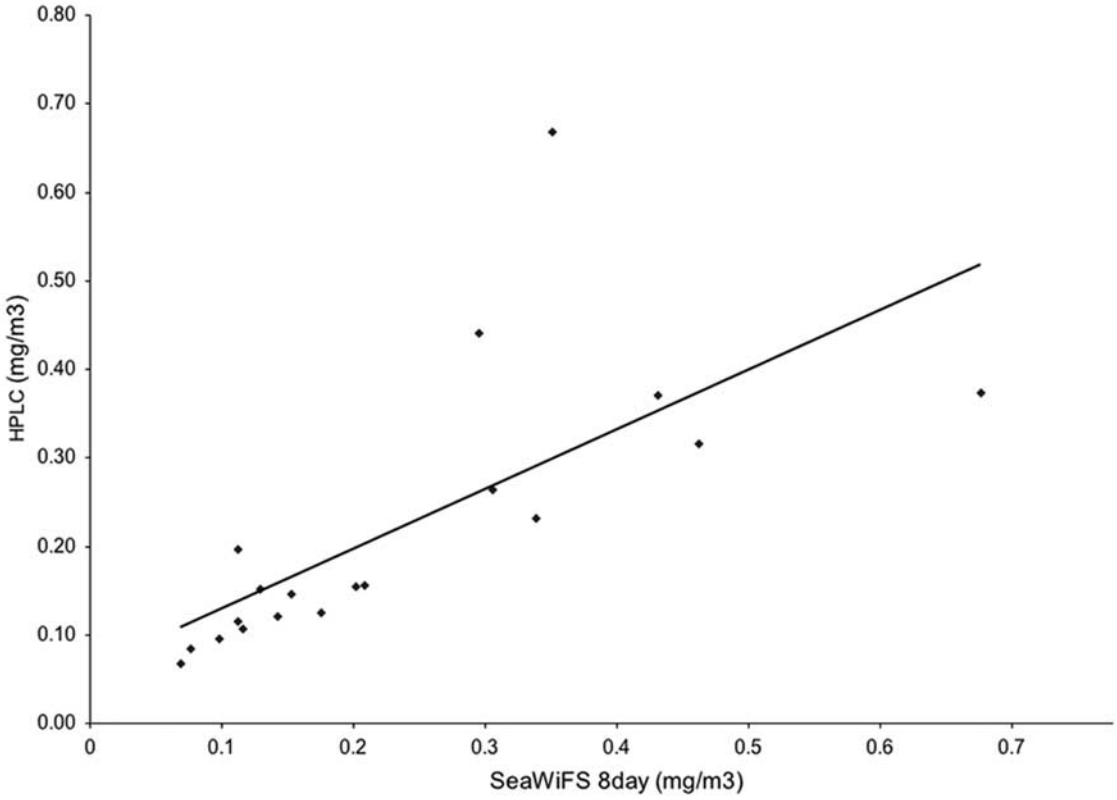

Figure 2. Relationship between chlorophyll *a* estimates obtained using HPLC of samples from Two Rocks stations B-E and ocean-color-derived estimates from SeaWiFS satellite observations.

21562202c, 2008, C7, Downloaded from https://agupubs.onlinelibrary.wiley.com/doi/10.1029/2007JC004102 by Cochrane France, Wiley Online Library on [31/05/2023]. See the Terms and Conditions (https://onlinelibrary.wiley.com/terms-and-conditions) on Wiley Online Library for rules of use; OA articles are governed by the applicable Creative Commons License

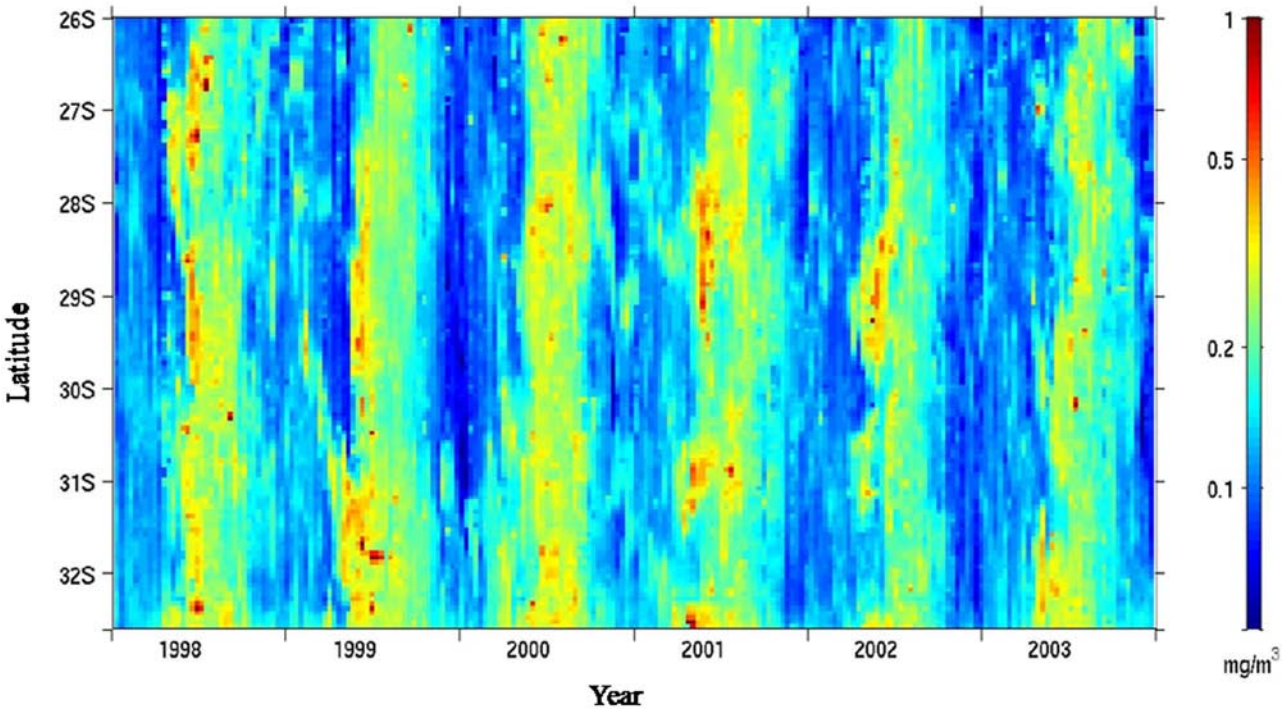

Figure 3. Distribution of chlorophyll estimated from SeaWiFS ocean color data along the shelf break off the west coast of Western Australia from 26°S–32°S, 1998–2003.

column, the nutrient and chlorophyll profile, and the micro and mesozooplankton. The community structure, seasonal cycle and grazing dynamics of the zooplankton will be described in subsequent papers.

2. Methods

[10] Our analysis combines satellite and in situ data sets to describe the spatial and temporal evolution of phytoplankton off the WA coast.

2.1. Satellite Data

[11] The satellite data sets of ocean color, sea-surface temperature ()SST and sea-surface height (SSH) were used to provide a larger-scale perspective (both spatially and temporally) to the study.

[12] The ocean color products were derived from the Sea-Viewing Wide-Field-of-View Sensor (SeaWiFS) using 8-d composites produced from GAC (Global Area Coverage) data with a nominal spatial resolution of 9 km. We also analyzed a set of 1 km resolution daily LAC (Local Area Coverage) SeaWiFS data.

[13] Thermal infrared data from the NOAA Advanced Very High Resolution Radiometer (AVHRR) provided a SST product. The AVHRR data product has a resolution of 10 d and 5 km and was derived from daily passes. The altimetry product used was a gridded data set of sea level anomalies from the Archiving, Validation, and Interpretation of Satellites Oceanographic Maps of Sea Level Anomalies (AVISO MSLA) Topex/Poseidon-ERS. The SSH time series covers January 1993 through December 2002. The altimeter data have a 7-d temporal resolution altimeter sea level anomaly product on a 1/3° Mercator grid based [*Ducet et al.*, 2000].

2.2. Field Data

[14] An onshore-offshore transect was established perpendicular to the coast approximately 50 km north of Perth, extending from an area known as Two Rocks across the continental shelf and out to 1000 m depth over the conti-

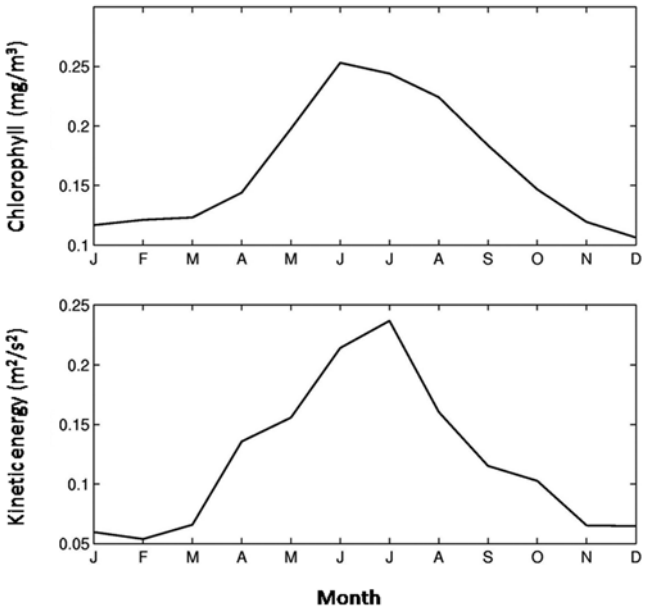

Figure 4. Climatological average for chlorophyll (upper) and eddy kinetic energy (lower) in the Leeuwin Current along the coast of Western Australia. The chlorophyll was estimated from the data in Figure 2 and the eddy kinetic energy from satellite altimetry.

21562202c, 2008, C7, Downloaded from https://agupubs.onlinelibrary.wiley.com/doi/10.1029/2007JC004102 by Cochrane France, Wiley Online Library on [31/05/2023]. See the Terms and Conditions (https://onlinelibrary.wiley.com/terms-and-conditions) on Wiley Online Library for rules of use; OA articles are governed by the applicable Creative Commons License

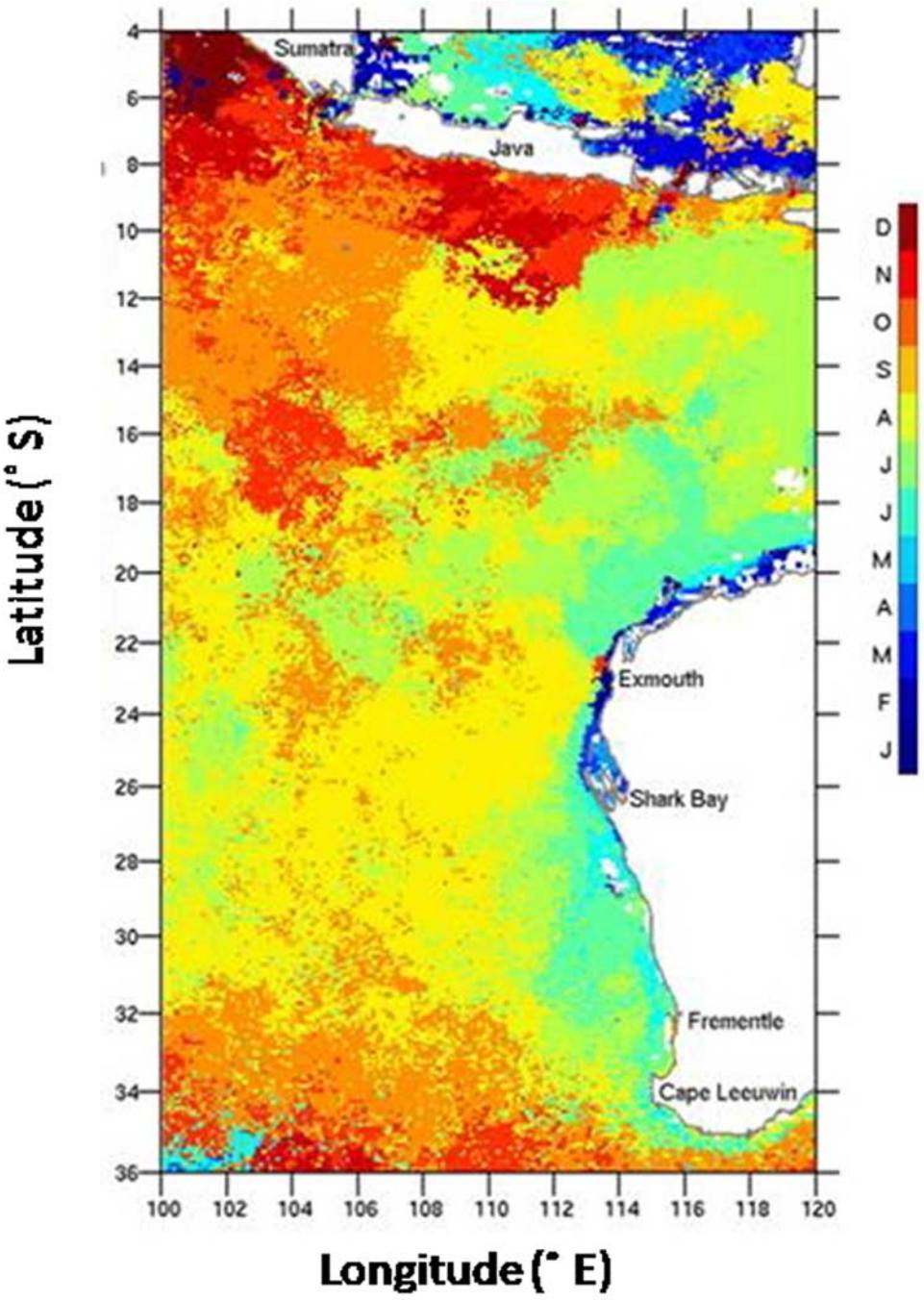

Figure 5. Climatology of phytoplankton production in the eastern Indian Ocean, showing the month of the peak chlorophyll *a* concentration as indicated from SeaWiFS ocean color data.

nental slope, about 100 km offshore. The transect position was selected to be typical of the open coast off southwestern Western Australia and to be beyond the influence of coastal outfalls, which enhance the local nutrient levels near Perth and of the Perth canyon and Rottnest island, which affect the local circulation [*Alaee et al.*, 1998; *Pearce et al.*, 2006].

[15] On a monthly basis, stations were occupied within the coastal lagoon (A: 15 m depth), on the inner shelf (B: 40 m), and on the outer shelf (C: 100 m) (Figure 1a and Table 1), using an 8-m shark cat. On a quarterly basis a larger vessel was chartered (the WA Fisheries vessel, *Naturaliste,* the TAFE training vessel, *Maritime Image,* or the Australian National Facility research vessel, *Southern Surveyor)* and stations at the shelf break (D: 300 m) and over the continental slope at the approximate outer edge of the Leeuwin Current (E: 1000 m) were occupied as well. Field sampling was carried out from February 2002 through December 2004, but cruises were sometimes missed, particularly during the first year, due to weather and mechanical breakdown. In all there were 27 cruises (Table 2).

[16] Conductivity-temperature-depth (CTD) casts were made at each station using a Seabird Model SBE 19+

21562202c, 2008, C7, Downloaded from https://agupubs.onlinelibrary.wiley.com/doi/10.1029/2007JC004102 by Cochrane France, Wiley Online Library on [31/05/2023]. See the Terms and Conditions (https://onlinelibrary.wiley.com/terms-and-conditions) on Wiley Online Library for rules of use; OA articles are governed by the applicable Creative Commons License

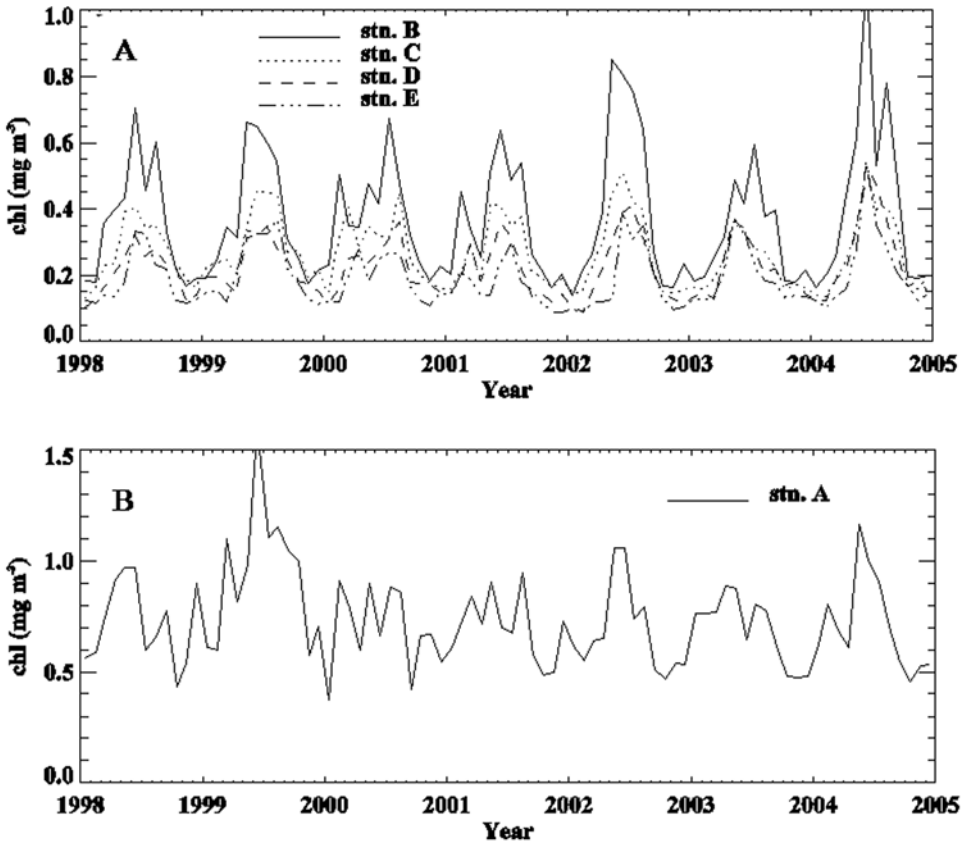

Figure 6. Monthly mean near-surface chlorophyll concentrations at the Two Rocks transect stations derived from daily SeaWiFS data between 1998 and 2004. (A) Data from stations B–E (40–1000 m depth); (B) data from station A (15 m depth within the coastal "lagoon"). See Figure 1a for locations of the stations.

instrument. A fluorometer, underwater quantum sensor to measure photosynthetically active radiation (PAR), and oxygen sensor were attached to the CTD, and the package was deployed on a rosette sampler equipped with 5 to 10 L Niskin bottles. CTD casts were made from surface down to near the seabed or to a maximum of 150 m in deeper water (with some occasional deeper casts, especially during the *Southern Surveyor* voyages). In order to improve the spatial resolution of physical data along the cross-shelf transect, CTD casts were carried out at additional stations (AB, BC, CD and DE) between the regular stations during the 2003 and 2004 quarterly cruises. Repeat casts (back to back or day versus night) were often made at regular stations during quarterly cruises. A total of 181 casts were made over the 3-year period.

[17] The CTD sampling frequency was 4 Hz, giving 4 samples per m depth interval at a lowering rate of 1 m s^{-1}. Standard Seabird software was used to process the raw CTD data and provide 1-m depth-averaged profiles which were used for all subsequent data analysis. Profile plots of all parameters were generated, followed by vertical sections to standardized length and depth scales.

[18] Water samples were collected at standard oceanographic depths, typically 1, 10, 25, 50, 75, 100, 150 m, and the depth of the fluorescence maximum. These were subsequently analyzed for salinity and dissolved macronutrients. Dissolved macronutrients were analyzed on a Lachat QuickChem Fluid Injection Analysis (FIA) 8000 series auto-analyzer using using Lachat QuickChem method 31-114-27-1-A (silicate), QuickChem method 31-107-04-1-A (nitrate + nitrite), and QuickChem method 31-115-01-1-G (phosphate). Ammonia was analyzed following the method of *Watson et al.* [2004]. OSIL reference standards were analyzed on every run.

[19] Chlorophyll *a* concentration (Chl*a*) was determined for all water samples collected within the euphotic zone. Water samples (0.5–2 L) were filtered under low vacuum (<100 mm Hg) onto 25 mm diameter glass fiber filters (Whatman GF/F^{TM}; nominal mesh size = 0.7 μm) and nylon

Table 3. Correlations (r) of the Integrated Chlorophyll-*a* Values at Stations A–E (see Table 1) and Number of Data Values (n)[a]

Station		A	B	C	D	E
A	r		0.444	0.228	0.082	0.097
	n		21	22	10	13
B	r	*		0.566	0.393	0.583
	n			20	10	10
C	r	ns	**		0.599	0.824
	n				10	12
D	r	ns	ns	*		0.497
	n					10
E	r	ns	*	**	?	

[a]One-tailed probability levels: ** $p < 0.01$; * $p < 0.05$; ?: $p < 0.10$.

21562202c, 2008, C7, Downloaded from https://agupubs.onlinelibrary.wiley.com/doi/10.1029/2007JC004102 by Cochrane France, Wiley Online Library on [31/05/2023]. See the Terms and Conditions (https://onlinelibrary.wiley.com/terms-and-conditions) on Wiley Online Library for rules of use; OA articles are governed by the applicable Creative Commons License

Table 4. Contribution of Each Station to the First Two Principal Components[a]

	Principal Component	
Station	1	2
A	0.379	0.874
B	0.793	0.333
C	0.906	−0.166
D	0.712	−0.320
E	0.865	−0.251

[a]The principal component analysis was based on the integrated chlorophyll-*a* values at each station along the Two Rocks transect (see Table 1).

textile disks (Nitex™; nominal mesh size = 5 μm). Immediately after filtration, filters were stored at −20°C until later analysis in the lab, where pigment retained on GF/F™ and Nitex™ disks was extracted in 8 mL of 90% acetone over night in the dark at 4°C. Pigments concentrations were measured using a Turner Designs model TD 700™ fluorometer and chlorophyll *a* was calculated following standard methods [*Parsons et al.*, 1984]. Chlorophyll *a* determined from particulate matter retained on the Nitex™ disks is indicative of large size (>5 μm) phytoplankton biomass (B_L), whereas that determined from particulate matter retained on the GF/F™ filters is indicative of total phytoplankton biomass (B_T). Chlorophyll *a* biomass of small size (<5 μm) phytoplankton (B_S) is obtained by subtracting the large size-fraction from total, i.e., $B_S = B_T - B_L$.

[20] Primary production was determined for six depths within the euphotic zone, including surface and the depth of maximum fluorescence, using the 14C uptake method [*Parsons et al.*, 1984]. Well-mixed samples were poured into one dark and two clear 140 ml-polycarbonate bottles (duplicate experiments) to which 20 μCi of $NaH^{14}CO_3$ were added. Time zero activity was determined from a subset of all incubation bottles by extracting a 100 μL aliquot and measuring ^{14}C in a scintillation counter onboard when possible or back in the lab. Bottles were incubated on deck from dawn-to-dawn (24 h) in a series of Plexiglas tubes covered with a range of blue and neutral films that simulate the intensity and nature of the underwater light field within the euphotic zone. Shade cloths were used to further reduce the light intensity when necessary. Thus the different irradiance levels simulated by the incubator were 100, 63, 38, 15, 5, 1, 0.3 or 0% (dark) of subsurface irradiance. Seawater pumped from ∼5 m below surface filled the incubator tubes and flowed continuously under pressure to keep samples at near-in situ temperature. Incubations were terminated in the dark by pouring the content of each incubation bottle through a 25 mm diameter disk of nylon textile (Nitex™ mesh size = 5 μm) and a Whatman GF/F™ filter placed in series. The filters were dropped into separate borosilicate vials and HCl was added on the filters (250 μl of 0.5 N) in order to remove nonincorporated ^{14}C. Vials were left open in a fume hood overnight or until the HCl had evaporated and the filters were dry. The activity was measured on a LKB RackBeta™ after adding 10 mL of scintillation cocktail. Carbon uptake was calculated according to *Parsons et al.* [1984] using a value of 26,900 mg C m^{-3} for the concentration of dissolved inorganic carbon.

[21] In the present paper, primary production is net (as opposed to gross) of the release of synthesized organic carbon into dissolved inorganic carbon (i.e., respiration) and dissolved organic carbon (i.e., exudation and cell lysis). The activity measured on the Nitex™ disks and the GF/F™ filters corresponds to the synthesis of particulate organic carbon by organisms in the large-size (P_L) and small-size (P_S) fractions, respectively. Total particulate carbon uptake (P_T) is obtained by adding the uptake of the two size fractions, i.e., $P_T = P_L + P_S$.

[22] Profiles of in situ fluorescence (in volts) were converted to chlorophyll *a* (in mg m^{-3}) using a regression (Chl*a* = −0.0361 + 1.1636*fluorescence) determined using data from all cruises.

[23] To examine the role of water column stratification on the vertical distribution of nutrients and primary production, we defined a "Gross Stratification Index" (GSI) as the difference between the near-surface (5 m) and bottom densities divided by the depth interval and multiplied by 100 (effectively a modified mean density gradient).

3. Results

3.1. Phytoplankton Biomass

[24] The SeaWiFS data used for the chlorophyll climatology were based on open ocean "case 1" algorithms. These can over-estimate chlorophyll in the presence of colored dissolved organic matter (CDOM) and suspended materials. The SeaWiFS sensor signal is weighted to the near surface layer and observes only the first optical depth. This limits SeaWIFS chlorophyll estimates to an average over a depth at which 90% of the backscattered irradiance is returned, roughly 22% of the euphotic zone [*Smith*, 1981].

[25] We investigated whether we could favorably compare the SeaWiFS-derived seasonal cycle on the central WA

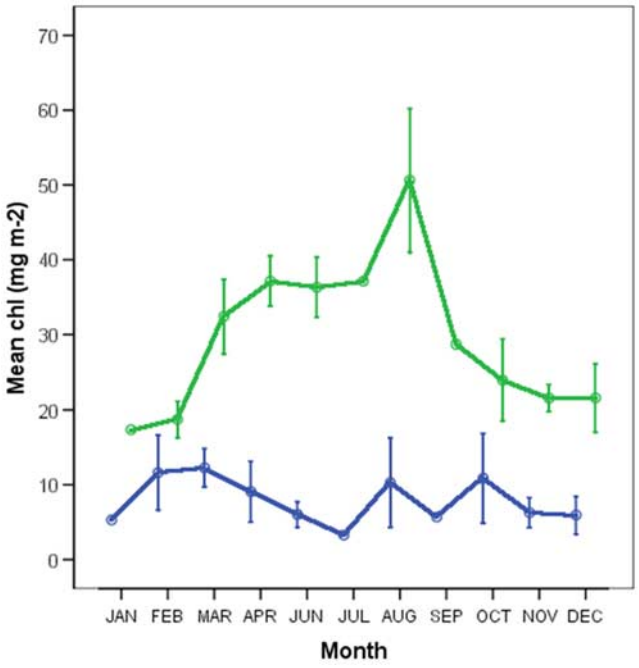

Figure 7. Mean integrated chlorophyll *a* from stations B–E (green) and station A (blue), across the Two Rocks transect, 2002–2004. Error bars are ±1 standard error. There were no data for May.

21562202c, 2008, C7, Downloaded from https://agupubs.onlinelibrary.wiley.com/doi/10.1029/2007JC004102 by Cochrane France, Wiley Online Library on [31/05/2023]. See the Terms and Conditions (https://onlinelibrary.wiley.com/terms-and-conditions) on Wiley Online Library for rules of use; OA articles are governed by the applicable Creative Commons License

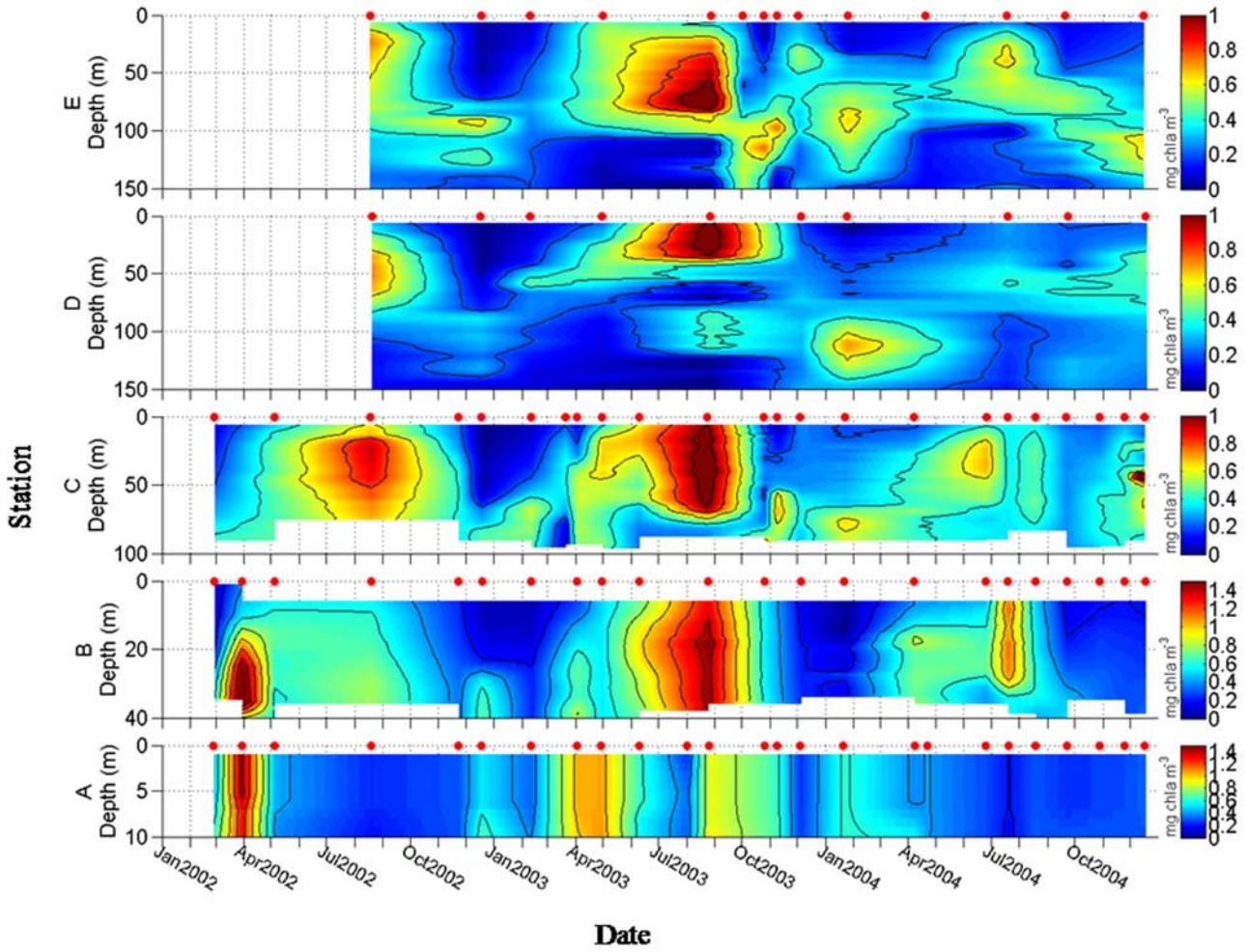

Figure 8. Time series of chlorophyll *a* (mg m^{-3}) at Two Rocks transect stations A to E, 2002–2004. Note the variable depth scale.

21562202c, 2008, C7, Downloaded from https://agupubs.onlinelibrary.wiley.com/doi/10.1029/2007JC004102 by Cochrane France, Wiley Online Library on [31/05/2023]. See the Terms and Conditions (https://onlinelibrary.wiley.com/terms-and-conditions) on Wiley Online Library for rules of use; OA articles are governed by the applicable Creative Commons License

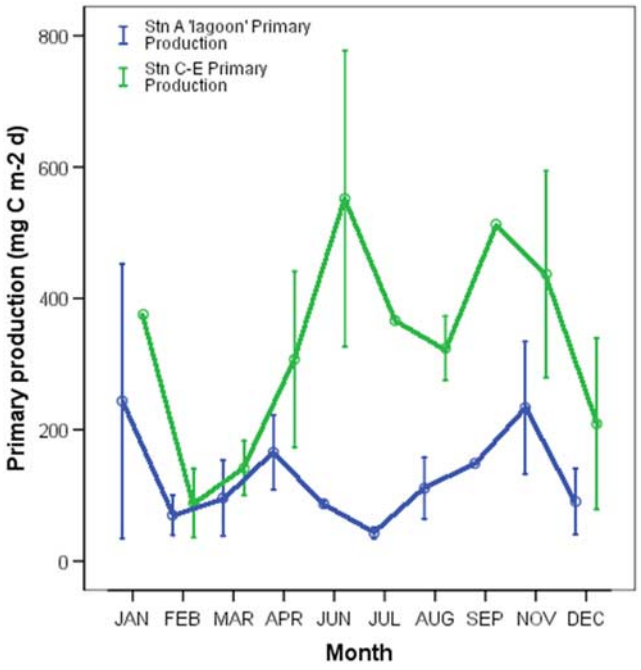

Figure 9. Mean monthly integrated primary production (±1 SE) at stations A (coastal "lagoon": 15 m) (blue), C (midshelf: 100 m) and E (outer Leeuwin Current: 1000 m) (green), 2002–2004.

shelf with surface in situ measurements from the Two Rocks transect. We excluded the very shallow 10 m station A, and plotted the scatter of HPLC-derived chlorophyll for all stations against the nearest 8-d, 9 km (8D9K) SeaWiFS composite value (Figure 2).

[26] The regression of Two Rocks HPLC derived chlorophyll against the matching SeaWiFS estimate is $Chla_{HPLC} = 0.675 * Chla_{SEAWiFS} + 0.0617$, $r^2 = 0.50$, explaining half the variance. One cause of error is inherent in matching a 9km, 8 d composite with an instantaneous in situ measurement made in a dynamic, mesoscale-influenced environment. If, for example, one of the outliers, where $Chla_{HPLC}$ is nearly twice the surface chlorophyll of the SeaWiFS estimate, is removed, the variance explained by the relationship increases to nearly 70%. Other causes of variability in the relationship include the influence of coastal "case 2" waters and the associated overestimates in remotely sensed chlorophyll. The average absolute match-up error between the nearest 8D9K SeaWiFS chlorophyll estimates and the HPLC measured chlorophyll *a* is 13% for the offshore stations, 36% for the shelf stations, and 95% for the 10 m depth nearshore station (not shown in figures). The mean absolute match-up errors for all but the nearshore station are of the same order of magnitude or less than the expected SeaWiFS match-up error for case-1 waters.

[27] The seasonal cycle of phytoplankton along the shelf break at the approximate core of the Leeuwin Current, based on chlorophyll concentration from 1998–2003 estimated from SeaWiFS ocean color data, shows a clear peak in late autumn or early winter, with moderately high chlorophyll levels persisting through the winter (Figure 3). Chlorophyll levels are minimal during the spring and summer. This cycle is broadly coherent off the coast of southwestern Western Australia from Shark Bay (26°S latitude) to Perth (32°S). Averaging these data to obtain the climatological average, the phytoplankton bloom, which occurs broadly over the months of April through June, coincides closely with the peak in the eddy kinetic energy of the Leeuwin Current, obtained from sea-height altimetry for this region (Figure 4).

[28] An examination of the timing of the phytoplankton bloom across the eastern Indian Ocean indicates that a late fall-early winter bloom is a distinct feature of the region over the continental shelf and within the Leeuwin Current from south of Shark Bay to Cape Leeuwin (Figure 5). The continental shelf north of Shark Bay exhibits a summer bloom, whereas offshore, chlorophyll peaks in later winter (August), as observed by *Humphrey* [1966]. The latter is consistent with the canonical oligotrophic subtropical gyre phytoplankton dynamics described by *Longhurst* [1998], in which winter cooling and increased wind mixing lead to a shoaling of the nutricline and a moderate winter bloom at latitudes where there is adequate light. The late fall-early winter bloom off southwestern Western Australia suggests that the region is subject to a distinct production regime, *sensu Longhurst* [1998], although this seasonal cycle and its dynamics are not described in that work.

[29] A more detailed examination of the SeaWiFS ocean color data along the Two Rocks transect across the continental shelf and Leeuwin Current (Stations B (40 m) – E (1000 m)) from 1998–2004 confirmed that the seasonal phytoplankton cycle was coherent onshore-offshore (Figure 6). However, peak concentrations of chlorophyll were higher at the inner shelf (40 m) station than farther offshore. The mean chlorophyll concentration at the inner shelf station in June was over 0.6 mg m^{-3}, falling to 0.2 mg m^{-3} in summer, whereas within the Leeuwin Current and offshore (stations D and E), the corresponding values were 0.3–0.4 mg m^{-3} in winter and about 0.1 mg m^{-3} in summer. This pattern is similar to that observed by *Pearce et al.* [2000] for the inner shelf off Hillarys just north of Perth.

[30] The chlorophyll data for the inshore station (A) at 15 m depth were more variable and not coherent with the data for the shelf and Leeuwin Current, although it is unclear from the satellite data alone whether this is because, at 15 m depth, the inshore data are biased by Case 2 water effects (Figure 6). Still, the broad outlines of a similar phytoplankton cycle are discernible, with a minimum chlorophyll concentration in spring and summer and peaks in autumn and winter.

[31] Field observations along the Two Rocks transect were consistent with the satellite data. Integrated chlorophyll *a* values over the study period were generally correlated ($0.4 < r < 0.8$) from the inner shelf to slope stations (B–E), whereas the chlorophyll *a* concentrations at the "lagoon" station were only significantly correlated with values at the adjacent inner shelf station (Table 3). Principal component analysis confirmed this pattern. The first two principal components explained 78% of the variance of the integrated chlorophyll *a* data set. The stations from the inner shelf to slope (B–E) all contributed strongly (loadings > 0.7) to the first component, which explained 57% of the variance, whereas the second component consisted predominantly of the contribution of the nearshore station (A) (Table 4).

21562202c, 2008, C7, Downloaded from https://agupubs.onlinelibrary.wiley.com/doi/10.1029/2007JC004102 by Cochrane France, Wiley Online Library on [31/05/2023]. See the Terms and Conditions (https://onlinelibrary.wiley.com/terms-and-conditions) on Wiley Online Library for rules of use; OA articles are governed by the applicable Creative Commons License

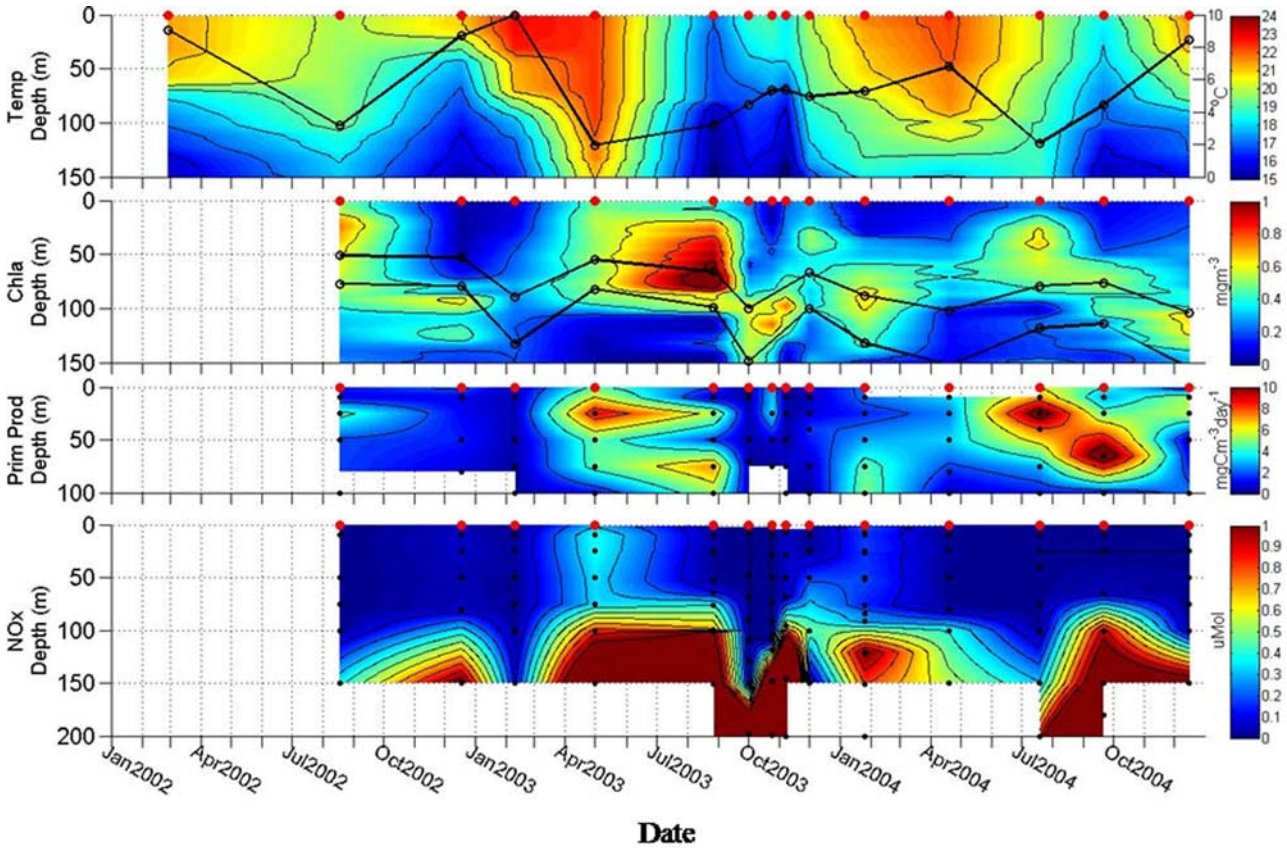

Figure 10. Time series (2002–2004) through the water column at station E (1000 m depth) in the outer Leeuwin Current, showing temperature (°C) (top), chlorophyll *a* (mg m^{-3}) (second from top), primary productivity (mg C m^{-3} d^{-1}) (third from top), and nitrate + nitrite (NOx) (μmole) (bottom). The line in the upper plots the Gross Stratification Index (GSI), and the lines in second panel indicate the depth of the 1% and 0.1% light levels.

21562202c, 2008, C7, Downloaded from https://agupubs.onlinelibrary.wiley.com/doi/10.1029/2007JC004102 by Cochrane France, Wiley Online Library on [31/05/2023]. See the Terms and Conditions (https://onlinelibrary.wiley.com/terms-and-conditions) on Wiley Online Library for rules of use; OA articles are governed by the applicable Creative Commons License

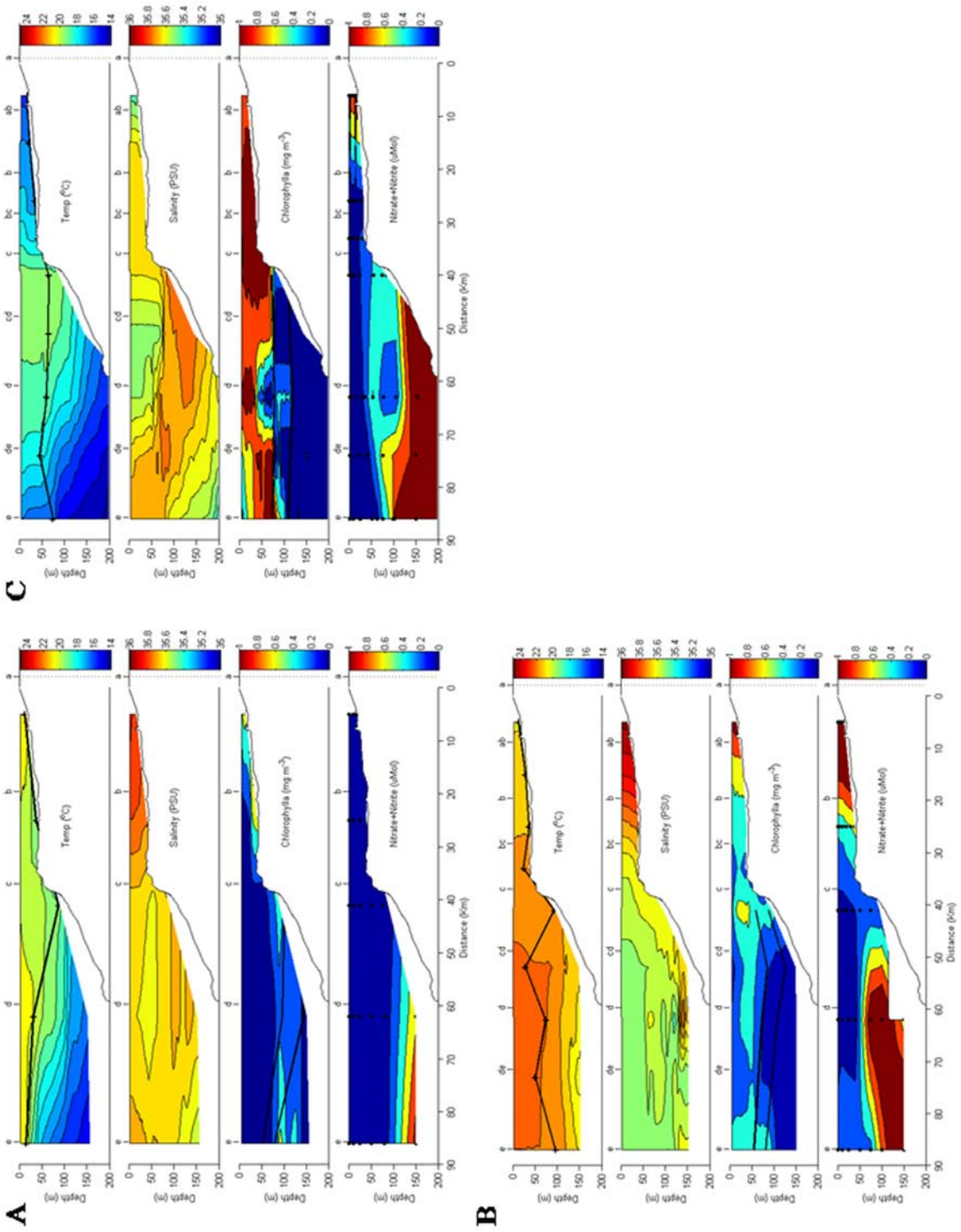

Figure 11. Sections showing temperature (°C), salinity (PSU), chlorophyll (mg m^{-3}), and nitrate + nitrite concentration (μmole) with depth across the Two Rocks transect during (A) summer (December 2002), (B) autumn (April 2003), and (C) winter (August 2003). The lines in the chlorophyll panels indicate the depth of the 1% and 0.1% light levels.

21562202c, 2008, C7, Downloaded from https://agupubs.onlinelibrary.wiley.com/doi/10.1029/2007JC004102 by Cochrane France, Wiley Online Library on [31/05/2023]. See the Terms and Conditions (https://onlinelibrary.wiley.com/terms-and-conditions) on Wiley Online Library for rules of use; OA articles are governed by the applicable Creative Commons License

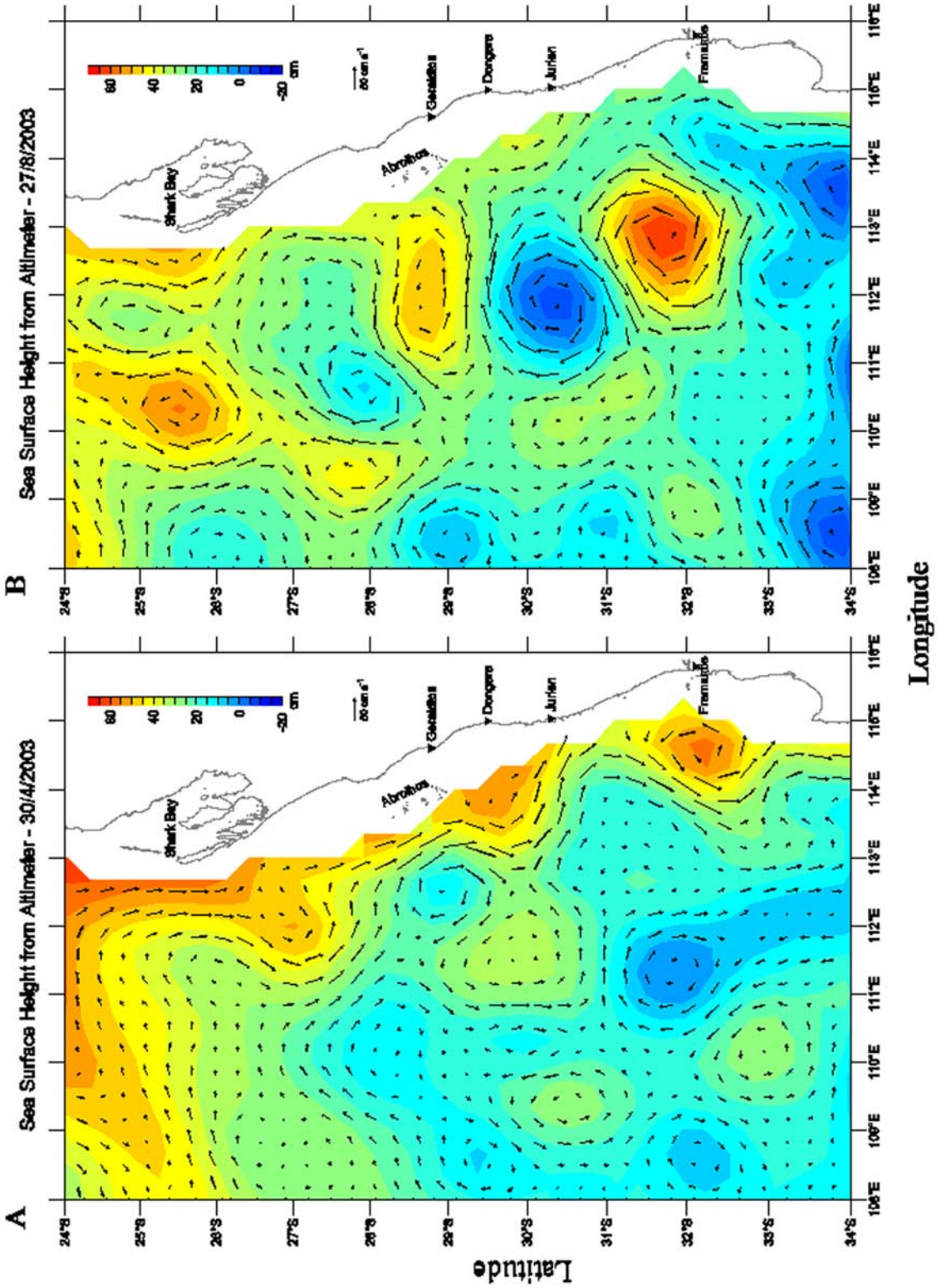

Figure 12. Sea-surface height from remotely sensed altimetry showing (A) an anticyclonic eddy offshore of the Two Rocks transect and a cyclonic meander just north of it on 30 April 2003, the time of the late autumn 2003 cruise, and (B) the cyclonic and anticyclonic eddy pair after it has detached from the Leeuwin Current and drifted westward into the Indian Ocean in winter (August 2003).

21562202c, 2008, C7, Downloaded from https://agupubs.onlinelibrary.wiley.com/doi/10.1029/2007JC004102 by Cochrane France, Wiley Online Library on [31/05/2023]. See the Terms and Conditions (https://onlinelibrary.wiley.com/terms-and-conditions) on Wiley Online Library for rules of use; OA articles are governed by the applicable Creative Commons License

[32] The field work across the Two Rocks transect, which provided data on the biomass of chlorophyll *a* integrated through the water column from the inner shelf to the slope (stations B–E), confirmed the satellite observations, indicating a broad autumn and winter maximum (March–September) with a minimum during austral spring and summer (October–February). There was approximately a factor of two difference in the integrated chlorophyll *a* concentration between these two periods ($mean_{(March-September)}$: 37.68 mg chl m^{-2}; $mean_{(October-February)}$: 20.66 mg chl m^{-2}; Figure 7). No clear seasonal cycle in chlorophyll concentration was observed at the inshore station.

[33] Although volumetric chlorophyll concentrations were higher inshore, the chlorophyll *a* integrated through the water column was consistently higher across the shelf and in the Leeuwin Current. These differences were greatest (a factor of 4.9: 37.68 mg chl m^{-2} offshore versus 7.76 mg chl m^{-2} inshore) during the autumn and winter, when chlorophyll concentrations were enhanced over the shelf and in the Leeuwin Current, but were still higher by a factor of 2.6 in the spring and summer.

[34] The vertical distribution of chlorophyll through the water column varied seasonally along with the changes in integrated chlorophyll concentration. Except for the lagoon station, the vertical distribution of chlorophyll from the inner shelf across the Leeuwin Current displayed a coherent seasonal pattern: in summer, a deep chlorophyll maximum at depths of about 75–125 m (or rising just above the seafloor in the inner shelf), which shoaled to depths of 0–70 m in late autumn and winter (Figure 8). During the bloom period, the chlorophyll layer across the shelf and Leeuwin Current intensified and thickened, often extending over about 50 m depth, as well as extending toward the surface.

3.2. Primary Production

[35] The seasonal patterns of primary production were similar to those of chlorophyll concentration but were less clear, possibly due in part to the fewer observations available of primary productivity (Figure 9). Primary production at the outer shelf and slope stations (C and E) was weakly correlated (Kendall's $\tau = 0.42$, $p < 0.05$), with highest primary production from late autumn to early spring offshore (station E) and extending into the summer on the shelf (station C). There was no well-defined seasonal cycle of productivity at the nearshore station. Primary production in autumn and winter was higher by a factor of 3.7 on the shelf and offshore ($mean_{April-September}$ = 412.49 mg C m^{-2} d^{-1}) than in the coastal lagoon (111.18 mg C m^{-2} d^{-1}), but was higher by only a factor of 1.6 during summer. Rates of primary production on the shelf and in the Leeuwin Current differed by about a factor of two between the autumn/winter and summer periods: $mean_{(April-September)}$: 412.49 mg C m^{-2} d^{-1} versus $mean_{(December-March)}$: 203.52 mg C m^{-2} d^{-1}.

[36] The seasonal cycle in chlorophyll *a* and primary productivity on the continental shelf and in the Leeuwin Current follows the seasonal cycle of stratification of the upper water column in summer and its de-stratification in late autumn and winter. This can be seen from the time series at Station E at the outer Leeuwin Current (Figure 10) and from cross-shelf sections undertaken during the various seasons (Figure 11). In summer, seasonal warming leads to the development of a relatively shallow mixed layer and highly stratified water column (Figures 10 and 11A). The Leeuwin Current is at a minimum, because it is flowing against the prevailing southerlies. The nutricline is at about 100 m depth, and the chlorophyll maximum layer is situated directly over it.

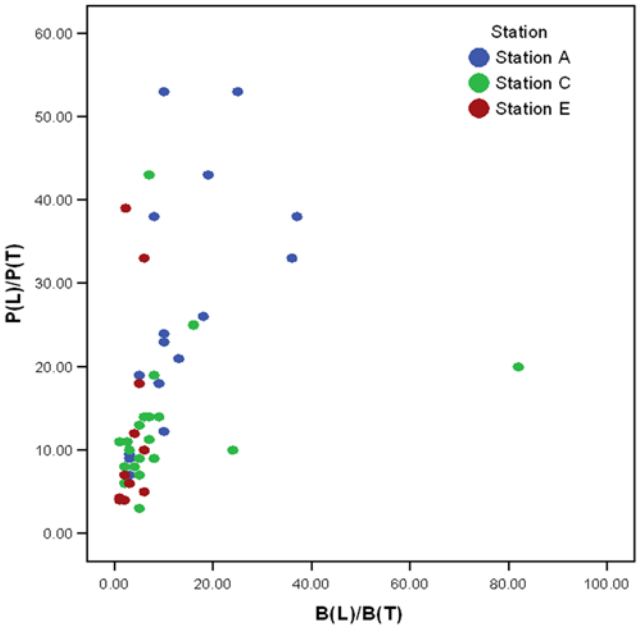

Figure 13. Relative proportion of "large-" sized phytoplankton (>5 um) to the total phytoplankton biomass (B_L/B_T) and production ((P_L/P_T) at the inshore (station A), midshelf (station C), and offshore (station E) stations along the Two Rocks transect.

[37] The late autumn and winter blooms appear to be initiated by two distinct mechanisms. The bloom observed in late April 2003 shows the influence of intensified Leeuwin Current flow and eddy activity (Figure 11B). Warm low-salinity Leeuwin water extended from offshore to the inner shelf to a depth of at least 150 m (the maximum depth of the CTD casts). The water column was weakly stratified, and the nutricline extended to about 50 m; measurable nitrate was recorded in near surface waters at the offshore station for the only time during the study (Figure 10). An anticyclonic eddy, which typically entrained the Leeuwin Current waters from the north [*Feng et al.*, 2007], formed just beyond the shelf break prior to this cruise. The offshore station (E) was within the eddy, and the predominance of Leeuwin water across the shelf appears to have been a product of the influence of the eddy and the cyclonic meander of the Leeuwin Current further upstream (Figure 12A).

[38] During winter bloom conditions, as encountered during August 2003, the physical structure of the water column differed markedly. The water column was destratified, again leading to a relatively shallow nutricline and shoaling and intensification of the chlorophyll layer, but destratification was due to the influence of winter cooling (Figure 11C), with the relatively warm, low-salinity core of the Leeuwin Current restricted to a shallow (<100 m) layer over the outer shelf due to relaxation of the Leeuwin Current

21562202c, 2008, C7, Downloaded from https://agupubs.onlinelibrary.wiley.com/doi/10.1029/2007JC004102 by Cochrane France, Wiley Online Library on [31/05/2023]. See the Terms and Conditions (https://onlinelibrary.wiley.com/terms-and-conditions) on Wiley Online Library for rules of use; OA articles are governed by the applicable Creative Commons License

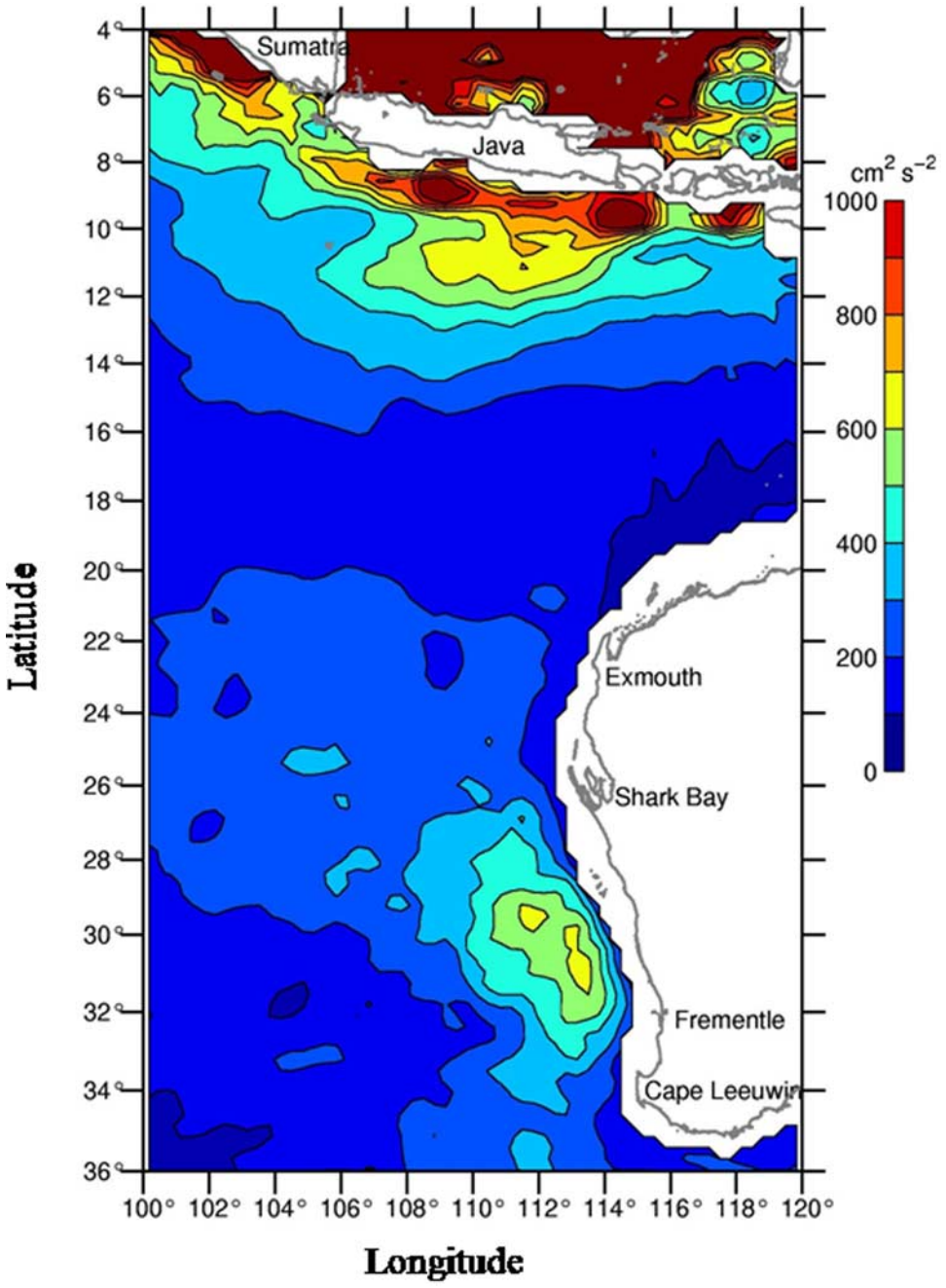

Figure 14. Distribution of eddy kinetic energy in the eastern Indian Ocean. Note the peak associated with Leeuwin Current eddies between the Abrolhos Islands, south of Shark Bay, and Cape Leeuwin.

after the eddies detached from the shelf (Figure 12B) [*Feng et al.*, 2007].

3.3. Phytoplankton Size Structure

[39] Phytoplankton <5 μm were responsible for most of the biomass and productivity across the Two Rocks transect (Figure 13), with a significant cross-shelf trend in the proportion of small phytoplankton comprising the total chlorophyll biomass: (means, stations A, C, E = 0.77, 0.91, 0.97, respectively; Friedman χ^2 = 6.68, $p < 0.05$). There was no significant trend in the proportion of primary production from the small phytoplankton size fraction across the shelf, with an overall mean of 82.60% of primary production derived from the small phytoplankton size fraction.

4. Discussion

[40] The canonical seasonal cycle in the oligotrophic subtropical ocean involves a summer period of water column stratification and low chlorophyll *a* levels integrated through the water column, with the phytoplankton concentrated in a deep chlorophyll maximum layer. Blooms are typically initiated when winter cooling and storm activity

21562202c, 2008, C7, Downloaded from https://agupubs.onlinelibrary.wiley.com/doi/10.1029/2007JC004102 by Cochrane France, Wiley Online Library on [31/05/2023]. See the Terms and Conditions (https://onlinelibrary.wiley.com/terms-and-conditions) on Wiley Online Library for rules of use; OA articles are governed by the applicable Creative Commons License

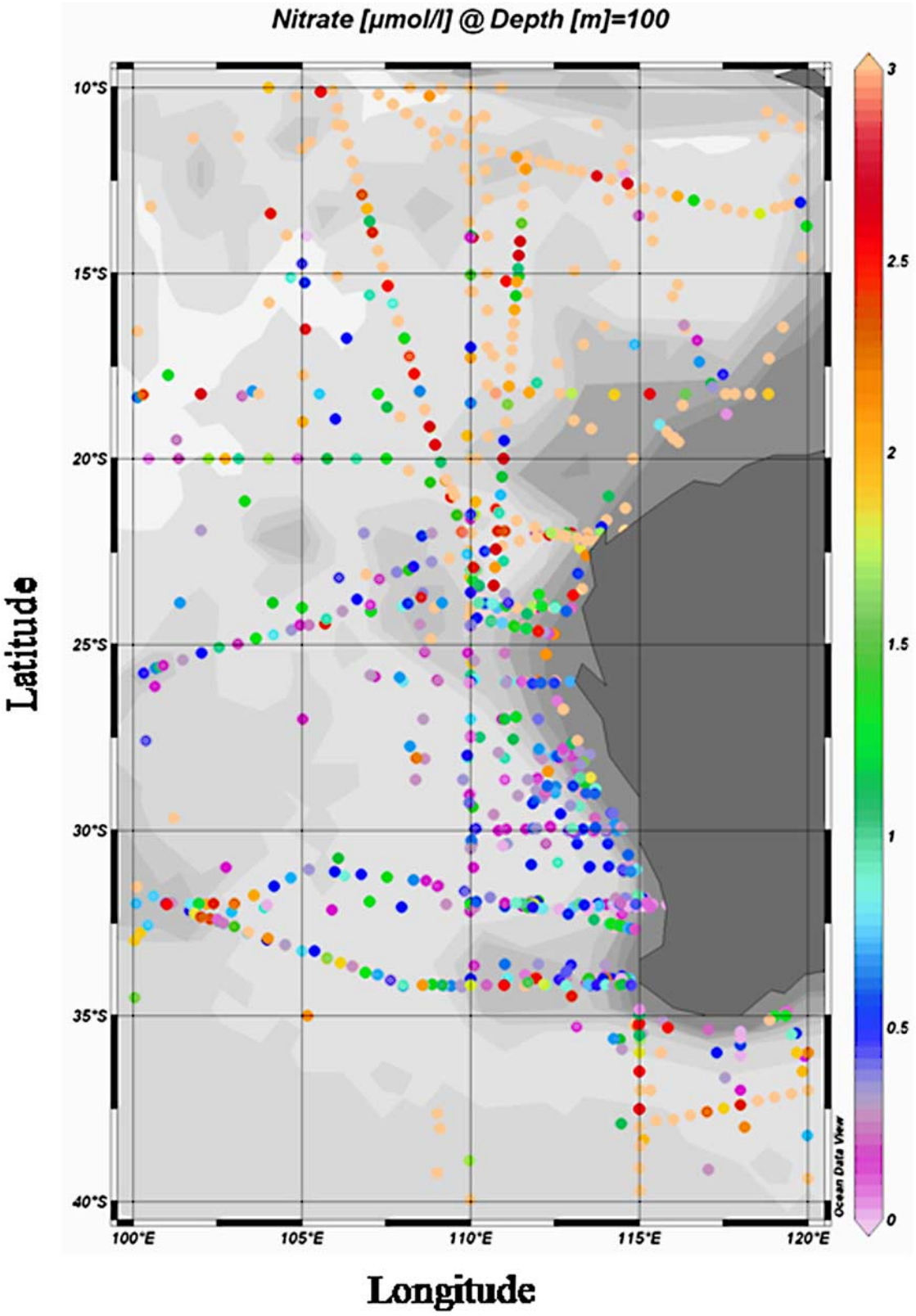

Figure 15. Nitrate concentrations at 100 m depth from the *Levitus and Boyer* [1994] historical database. Higher values are generally found in the tropical source waters of the Leeuwin Current.

21562202c, 2008, C7, Downloaded from https://agupubs.onlinelibrary.wiley.com/doi/10.1029/2007JC004102 by Cochrane France, Wiley Online Library on [31/05/2023]. See the Terms and Conditions (https://onlinelibrary.wiley.com/terms-and-conditions) on Wiley Online Library for rules of use; OA articles are governed by the applicable Creative Commons License

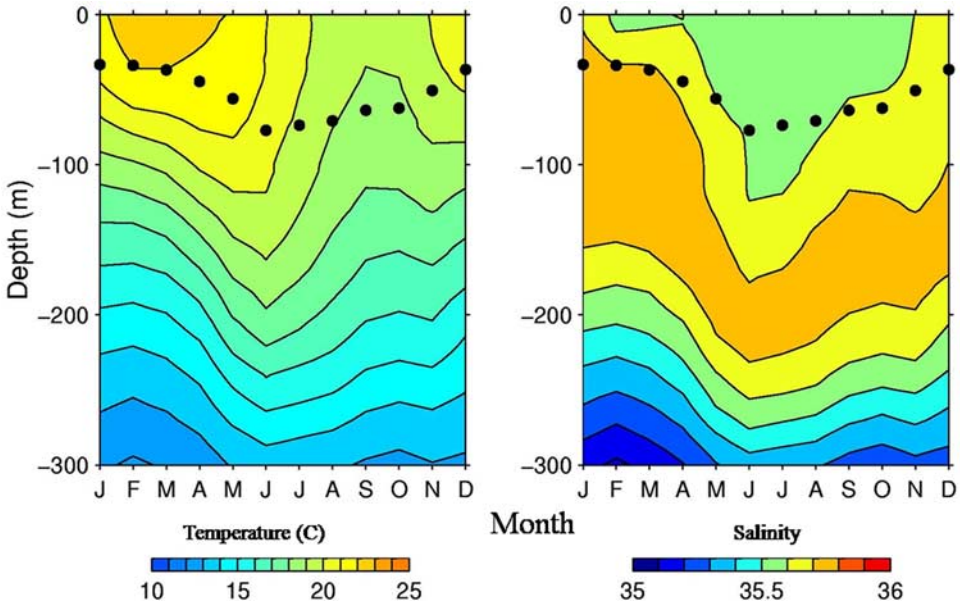

Figure 16. Vertical temperature and salinity sections for the upper 300 m at station E derived from the *Levitus and Boyer* [1994] climatology. The dots represent the monthly mixed layer depths.

destratify the water column, leading to convective mixing of nutrient into the euphotic zone [*Longhurst*, 1998]. The late autumn bloom initially appears anomalous because it is not associated with decreased near-surface temperatures: in fact the shelf was flooded with warm Leeuwin Current water in late April 2003 during the bloom (Figure 11). Nor is it associated with enhanced winds: mean wind speed decreases in autumn relative to summer off southwestern Western Australia, due to the decline in the summer monsoonal winds [*Pearce et al.*, 2006]. Neither is it possible that the autumn bloom is associated with runoff, which is negligible off central and southwestern Western Australia: the region's few, small rivers would not influence the oceanography over the continental shelf in autumn beyond the coastal "lagoon."

[41] The onset of the late autumn bloom over more than 700 km of the warm temperate-to-subtropical coast from south of Shark Bay to south of Perth (Figure 3) coincides temporally with the decline of the monsoonal southerlies and intensification of the Leeuwin Current (Figure 4) and spatially with the region of maximal eddy intensification (Figure 14). The Leeuwin Current has far higher eddy kinetic energy than any "typical," equatorward-flowing eastern boundary current [*Feng et al.*, 2005]. There are at least four mechanisms whereby eddies and enhanced flow of the Leeuwin Current may promote phytoplankton production.

[42] First, the eddy motion against the continental slope and shelf may directly upwell nutrients. That this may be happening is suggested by the shoreward uptilting of salinity and nutrient isopleths during the late April 2003 cruise when an eddy and meander pair were situated just beyond the shelf break, directly impinging on the outer stations on our transect (Figure 12A). Leeuwin Current water flooded the shelf during this cruise, indicating an exchange of water between the shelf and Leeuwin Current that appeared to advect relatively nutrient-rich water onto the shelf.

[43] A similar mechanism has been described for several western boundary currents, where eddies and meanders over the continental slope "pump" nutrients onto the continental shelf and thereby promote a significant proportion of the shelf productivity off the southeast USA [*Yoder et al.*, 1981; *Lee and Atkinson*, 1983; *Lee et al.*, 1989, 1991], Brazil [*Campos et al.*, 2000], Japan [*Kimura et al.*, 1997], and eastern Australia [*Tranter et al.*, 1986; *Harris et al.*, 1987]. The western boundary currents are often notably low in nutrients, yet the eddy and meander structures promote shelf productivity through eddy-induced upwelling along the shelf break, because the nitricline is lifted upward toward the continental shelf. More relevant to a poleward flowing eastern boundary current where the nitricline is depressed downward toward the continental shelf, a similar phenomenon has been observed along the outer shelf of the Bering Sea where the Bering Slope Current flows northeastward [*Stabeno and Meurs*, 1999; *Mizobata and Saitoh*, 2004]. Strong cross-shelf currents induced by eddies in the BSC were observed to bring high nutrient waters onto the shelf and drive ocean productivity [*Mizobata and Saitoh*, 2004]. Similar cross-shelf processes could occur in the Leeuwin Current system when the eddy energy is strengthened during austral autumn-winter, as observed during April 2003 (Figures 11 and 12A). Note that the occurrence of the late autumn phytoplankton bloom in April 2003 is not simultaneous along the shelf, as observed from satellite data (Figure 3). The nutrient enrichment and enhanced production are more likely observed in the anticyclonic structures downstream of the cyclonic meanders of the Leeuwin Current.

[44] Second, during this more vigorous phase of the Leeuwin's seasonal cycle, the current may advect nutrients from the north. The nutricline is shallower in the tropical source waters of the Leeuwin Current (Figure 15). As the flow of the Leeuwin Current is enhanced in late autumn, these deeper nutrients may be entrained into the Leeuwin Current and transported south.

21562202c, 2008, C7, Downloaded from https://agupubs.onlinelibrary.wiley.com/doi/10.1029/2007JC004102 by Cochrane France, Wiley Online Library on [31/05/2023]. See the Terms and Conditions (https://onlinelibrary.wiley.com/terms-and-conditions) on Wiley Online Library for rules of use; OA articles are governed by the applicable Creative Commons License

[45] The seasonal breakdown in stratification also likely contributes to the late autumn and winter blooms. A deepening thermocline in late autumn and winter can be seen in the climatology for the region of the offshore station on our transect (Figure 16), based on data from *Levitus and Boyer* [1994]. The climatology reveals that the thermocline deepens initially with the influx of low salinity Leeuwin water and remains relatively deep as the water column cools in winter: mixed layer depth increases from about 30 m in January/February to over 80 m in June. Stratification declines at the same time, the vertical temperature differential between the surface and 300 m dropping from about 11°C in summer to about 7°C in winter. The salinity structure shows both the low salinity of the Leeuwin Current tropical water near the surface in winter and the presence of high salinity (>35.9 psu) Indian Ocean Central Water at a depth of about 100 m in summer and deepening to almost 200 m in winter. The deepening of the mixed layer is driven by the strengthening of the Leeuwin Current before the start of winter (May–June). With the relaxation of the Leeuwin Current during the winter, decreased stratification appears to be a response to seasonal surface cooling which enhances convective mixing and entrains deep thermocline water into the mixed layer. These processes likely combine to enrich the Leeuwin Current waters during the winter period.

[46] At inner-to-mid shelf depths, regenerated nutrient from within the sediments may also be mixed into the water column by these processes, providing a further nutrient source for the seasonal bloom.

[47] The role of Leeuwin Current eddies in promoting productivity off southwestern Australia may explain the hitherto paradoxical positive correlation between the strength of the Leeuwin Current, hitherto considered a low-nutrient water mass, with recruitment to the western rock lobster (*Panulirus cygnus*). Further research will be required, however, to elucidate the mechanisms responsible for eddy enrichment of the continental shelf and the influence on the growth and survival of larvae of the western rock lobster and potentially of other key regional species.

[48] **Acknowledgments.** We acknowledge the assistance of many persons with the field program, in particular M. Harrison, N. Mortimer, and N. Johnston. Nick Mortimer assisted with the database and graphics. Funding was provided by the Strategic Research Fund for the Marine Environment (SRFME), a joint venture between CSIRO and the government of Western Australia.

References

Alaee, M. J., C. B. Pattiaratchi, and G. Ivey (1998), A field study of the three-dimensional structure of the Rottnest Island wake, in *Physics of Estuaries and Coastal Sea*, edited by A. Dronkers and A. Scheffers, pp. 239–245, Balkema, Rotterdam.

Birol, F., and R. Morrow (2001), Source of the baroclinic waves in the southeast Indian Ocean, *J. Geophys. Res.*, *106*, 9145–9160.

Campos, E. J. D., D. Velhote, and I. C. A. Da Silveira (2000), Shelf break upwelling driven by Brazil current cyclonic meanders, *Geophys. Res. Lett.*, *27*, 751–754.

Caputi, N., C. Chubb, and A. Pearce (2001), Environmental effects on recruitment of the western rock lobster, *Panulirus Cygnus*, *Mar. Freshwater Res.*, *52*, 1167–1174.

Cresswell, G. R. (1991), The Leeuwin Current: Observations and recent models, *J. R. Soc. West. Aust.*, *74*, 1–14.

Cresswell, G. R., and T. J. Golding (1980), Observations of a south-flowing current in the southeastern Indian Ocean, *Deep Sea Res., Part I or Part II*, *27*, 449–466.

Ducet, N., P.-Y. Le Traon, and G. Reverdin (2000), Global high resolution mapping of ocean circulation from TOPEX/Poseidon and ERS-1/2, *J. Geophys. Res.*, *105*, 19,477–19,498.

Fang, F., and R. Morrow (2003), Evolution and structure of Leeuwin Current eddies in 1995–2000, *Deep Sea Res.*, *II 50*, 2245–2261.

Feng, M., G. Meyers, A. Pearce, and S. Wijffels (2003), Annual and interannual variations of the Leeuwin Current at 32°S, *J. Geophys. Res.*, *108*(C11), 3355, doi:10.1029/2002JC001763.

Feng, M., S. Wijffels, S. Godfrey, and G. Meyers (2005), Do eddies play a role in the momentum balance of the Leeuwin Current?, *J. Phys. Oceanogr.*, *35*, 964–975.

Feng, M., L. Majewski, C. Fandry, and A. Waite (2007), Characteristics of two counter-rotating eddies in the Leeuwin Current system off the Western Australian coast, *Deep Sea Res.*, *II 54*, 961–980.

Gaughan, D., and T. Leary (2003), West coast purse seine managed fishery status report, in *State of the Fisheries Report*, pp. 38–40, Department of Fisheries, Western Australia.

Godfrey, J. S., and K. R. Ridgway (1985), The large-scale environment of the poleward-flowing Leeuwin Current, Western Australia: Longshore steric height gradients, wind stresses and geostrophic flow, *J. Phys. Oceanogr.*, *15*, 481–495.

Griffin, D. A., J. L. Wilkin, C. F. Chubb, A. F. Pearce, and N. Caputi (2001), Ocean currents and the larval phase of Australian western rock lobster, *Panulirus Cygnus*, *Mar. Freshwater Res.*, *52*, 1187–1199.

Harris, G., C. Nilsson, L. Clementson, and D. Thomas (1987), The water masses of the east coast of Tasmania: Seasonal and interannual variability and the influence on phytoplankton biomass and productivity, *Aust. J. Mar. Freshwater Res.*, *38*, 569–590.

Humphrey, G. F. (1966), The concentration of chlorophylls a and c in the south-east Indian Ocean, *Austr. J. Mar. Freshwater Res.*, *17*, 135–145.

Kimura, S., A. Kasai, H. Nakata, T. Sugimoto, J. H. Simpson, and J. V. S. Cheok (1997), Biological productivity of mesoscale eddies caused by frontal disturbances in the Kuroshio, *ICES J. Mar. Sci.*, *54*, 179–192.

Lee, T. N., and L. P. Atkinson (1983), Low-frequency current and temperature variability from Gulf Stream frontal eddies and atmospheric forcing along the southeast outer continental shelf, U.S., *J. Geophys. Res.*, *88*, 4541–4567.

Lee, T. N., E. Williams, J. Wang, R. Evans, and L. P. Atkinson (1989), Response of South Carolina continental shelf waters to wind and Gulf Stream forcing during winter of 1986, *J. Geophys. Res.*, *94*, 10,715–10,754.

Lee, T. N., J. A. Yoder, and L. P. Atkinson (1991), Gulf Stream frontal eddy influence on productivity of the southeast continental shelf, U.S., *J. Geophys. Res.*, *96*, 22,191–22,205.

Lenanton, R. C., L. Joll, J. Penn, and K. Jones (1991), The influence of the Leeuwin Current on coastal fisheries of Western Australia, *J. R. Soc. West. Aust.*, *74*, 101–114.

Levitus, S., and T. P. Boyer (1994), *World Ocean Atlas*, vol. 4: *Temperature*, *NOAA Atlas NESDIS 4*, 117 pp., U.S. Dept. of Commerce, Washington, D.C., USA.

Longhurst, A. (1998), *Ecological Geography of the Seas*, Acadamic Press, San Diego.

Lourey, M. J., J. R. Dunn, and J. Waring (2006), A mixed-layer nutrient climatology of Leeuwin Current and Western Australian shelf waters: Seasonal nutrient dynamics and biomass, *J. Mar. Syst.*, *59*, 25–51.

Mizobata, K., and S. Saitoh (2004), Variability of Bering Sea eddies and primary productivity along the shelf edge during 1998–2000 using satellite multisensor remote sensing, *J. Mar. Syst.*, *50*, 101–111.

Moore, T. S. (2005), Physical oceanographic controls on phytoplankton distribution in the Banda Sea and Western Australian region, Ph.D. dissertation, University of Tasmania, Hobart, Australia.

Morrow, R., F. Fang, M. Fieux, and R. Molcard (2003), Anatomy of three warm-core Leeuwin Current eddies, *Deep Sea Res.*, *II 50*, 2229–2243.

Parsons, T. R., Y. Maita, and C. M. Lalli (1984), *A Manual of Chemical and Biological Methods for Seawater Analysis*, 187 pp., Pergamon Press, Oxford.

Pearce, A. (1991), Eastern boundary currents of the southern hemisphere, *J. R. Soc. West. Aust.*, *74*, 35–45.

Pearce, A., and C. Pattiaratchi (1999), The Capes Current: A summer countercurrent flowing past Cape Leeuwin and Cape Naturaliste, Western Australia, *Cont. Shelf Res.*, *19*, 401–420.

Pearce, A., S. Helleren, and M. Marinelli (2000), Review of productivity levels of Western Australian coastal and estuarine waters for mariculture planning purposes, in *Fisheries Research Report 123*, 57 pp., Fisheries Western Australia Perth, Australia.

Pearce, A. F., M. J. Lynch, and C. E. Hanson (2006), The Hillarys transect (1): Seasonal and cross-shelf variability of physical and chemical water properties off Perth, Western Australia, 1996–98, *Cont. Shelf Res.*, *26*, 1689–1729.

21562202c, 2008, C7, Downloaded from https://agupubs.onlinelibrary.wiley.com/doi/10.1029/2007JC004102 by Cochrane France, Wiley Online Library on [31/05/2023]. See the Terms and Conditions (https://onlinelibrary.wiley.com/terms-and-conditions) on Wiley Online Library for rules of use; OA articles are governed by the applicable Creative Commons License

Potemra, J. T. (2001), Contribution of equatorial Pacific winds to southern tropical Indian Ocean Rossby waves, *J. Geophys. Res.*, *106*, 2407–2422.

Ridgway, K. R., and S. A. Condie (2004), The 5500-km-long boundary flow off western and southern Australia, *J. Geophys. Res.*, *109*, C04017. doi:10.1029/2003JC001921.

Smith, R. C. (1981), Remote sensing and depth distribution of ocean chlorophyll, *Mar. Ecol. Prog. Ser.*, *5*, 359–361.

Smith, R. L., A. Huyer, J. S. Godfrey, and J. A. Church (1991), The Leeuwin Current off Australia, 1986–1987, *J. Phys. Oceanogr.*, *21*, 323–345.

Stabeno, P. J., and V. Meurs (1999), Evidence of episodic on-shelf flow in the southeastern Bering Sea, *J. Geophys. Res.*, *104*, 29,715–29,720.

Sverdrup, H. U. (1953), On the conditions for vernal blooming of the phytoplankton, *J. Cons. Int. Explor. Mer*, *18*, 287–295.

Thompson, P., and A. Waite (2003), Phytoplankton responses to wastewater discharge at two sites in Western Australia, *Mar. Freshwater Res.*, *54*, 721–735.

Tranter, D. J. (1977), Further studies of plankton ecosystems in the eastern Indian Ocean. part I: Introduction - The study and the study area, *Aust. J. Mar. Freshwater Res.*, *28*, 529–539.

Tranter, D. J., D. J. Carpenter, and G. S. Leech (1986), The enrichment effect of the east Australian current eddy field on the central coast of New South Wales, *Deep Sea Res.*, *33*, 1705–1728.

Watson, R. J., E. C. V. Butler, L. A. Clementson, and K. M. Berry (2004), Flow-injection analysis with fluorescence detection for the determination of trace levels of ammonium in seawater, *J. Environ. Monit.*, doi:10.1039/b405924g.

Yoder, J. A., L. P. Atkinson, T. N. Lee, H. H. Kim, and C. R. McClain (1981), Role of Gulf Stream frontal eddies in forming phytoplankton patches on the outer southeastern shelf, *Limnol. Oceanogr.*, *26*, 1103–1110.

Yoder, J. A., C. R. McClain, G. C. Feldman, and W. Esaias (1993), Annual cycles of phytoplankton chlorophyll concentrations in the global ocean: a satellite view, *Global Biogeochem. Cycles*, *7*, 181–193.

P. Fearns, M. Feng, and A. Pearce, CSIRO Marine and Atmospheric Research, Private Bag 5, Wembley, WA 6913, Australia.

J. A. Koslow, Integrative Oceanography Division, Scripps Institution of Oceanography, University of California, San Diego, La Jolla, CA 92093-0218, USA. (tkoslow@ucsd.edu)

R. Matear and T. Moore, CSIRO Marine and Atmospheric Research, GPO Box 1538, Hobart, Tas 7001, Australia.

S. Pesant, Observatoire Océanologique, Laboratoire d'Océanographie de Villefranche (LOV) - UMR 7093, B.P. 28, 06234 Villefranche-sur-Mer, France.

A. Waite, School of Environmental Systems Engineering, University of Western Australia, 35 Stirling Highway, Crawley, WA 6009, Australia.

21562202c, 2008, C7, Downloaded from https://agupubs.onlinelibrary.wiley.com/doi/10.1029/2007JC004102 by Cochrane France, Wiley Online Library on [31/05/2023]. See the Terms and Conditions (https://onlinelibrary.wiley.com/terms-and-conditions) on Wiley Online Library for rules of use; OA articles are governed by the applicable Creative Commons License